Nanoscale Tailoring

DOI: 10.1002/anie.201007358

Fine Characteristics Tailoring of Organic and Inorganic Nanowires Using Focused Electron-Beam Irradiation**

*Young Ki Hong, Dong Hyuk Park, Seong Gi Jo, Min Ho Koo, Dae-Chul Kim, Jeongyong Kim, Joon-Sung Kim, Sung-Yeon Jang, and Jinsoo Joo**

Since the discovery of the superlattice structure,[1] 1D periodic arrangements, such as heterojunction nanowires (NWs), have been widely adopted for energy-band engineering techniques[2] and applications to optoelectronic nanodevices.[2b,3] Most heterojunction 1D nanomaterials comprise alternating sections of materials with distinct properties.[2a,3a,4]

Fabricating or tailoring various nanostructures using high-energy charged beams, such as electron beams (E-beams) or ion beams, has attracted considerable attention over the last few years.[5] For example, nanosculpting of graphene,[6] fabrication of low-dimensional optical nanopatterns or light-emitting nanostructures,[7] and the formation of hierarchical pore structures[8] have been achieved using an unfocused E-beam irradiator, scanning electron microscope (SEM), or transmission electron microscope (TEM) with energy levels of a few tens or hundreds of kiloelectronvolts.

The spot size and irradiating position of the focused E-beam can be controlled to achieve the desired accuracy and can be scaled down to the nanoscale. Therefore, the partial, intended, and separate compartments of nanomaterials can be modified. Nanoscale modification of intrinsic properties of nanomaterials is possible depending on the tunable energy and dose of the focused E-beam.

Herein, we report on focused E-beam irradiation techniques that can tailor precisely the optical and structural properties of both organic and inorganic semiconducting single NWs on the nanoscale. Light-emitting organic poly(3-methylthiophene) (P3MT) and inorganic titanium dioxide (TiO_2) single NWs have been tailored successfully to contain multiple 1D serial compartments, similar to a superlattice NW. These compartments have different lengths and characteristics, which can be modified precisely through treatment with a focused E-beam. Herein we examine the dramatic changes in the structural, optical, and electrical properties of compartments of single P3MT and TiO_2 NWs treated with a focused E-beam under different conditions. We suggest that focused E-beam treatment as a postsynthesis manipulation procedure is a promising technique for fine tailoring of the intrinsic properties of organic and inorganic nanosystems.

The spot size of the focused E-beam was controlled from 50 to 100 nm, and the step size of the focused E-beam irradiation was 2.4 nm (Scheme 1). The energy of the focused E-beam was fixed to 30 keV and its dose was controlled from 7.5×10^{16} to 1.0×10^{19} electrons cm^{-2}. The doses for the focused E-beam were approximately 10^2–10^4 times higher than those used in conventional E-beam lithography (for example, the dose of the electron resist for poly(methyl methacrylate) is ca. 10^{15} electrons cm^{-2}).

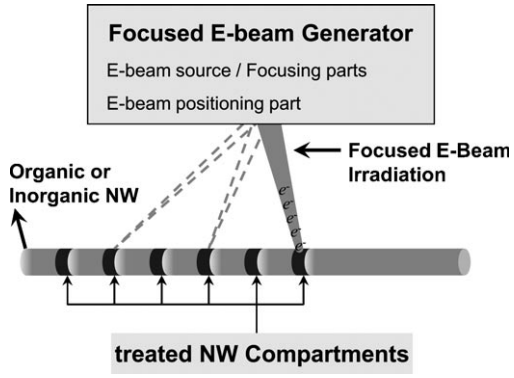

Scheme 1. Schematic diagram of the focused E-beam irradiation of designated positions of the organic or inorganic single NW.

Figure 1 shows the nanoscale optical properties of individual treated P3MT NWs measured by a color charge-coupled device (CCD) and laser confocal microscopy (LCM) photoluminescence (PL) experiments. The PL color of the pristine NW compartments in the P3MT NW remained at the original green with relatively low brightness. When designated positions of the single NW were irradiated with a focused E-beam with a dose of 7.5×10^{16} electrons cm^{-2}, the PL color of the treated NW compartments changed from green to yellow, and the emission intensity was clearly enhanced (Figure 1a). The LCM PL intensities of the treated compartments (dose $=7.5\times10^{16}$ electrons cm^{-2}) were approximately 12 times higher than those of the pristine P3MT NW (Figure 1b). When the dose was increased to 2.5×10^{17} electrons cm^{-2}, the PL color of the treated P3MT NW

[*] Dr. Y. K. Hong, Dr. D. H. Park, S. G. Jo, M. H. Koo, Prof. J. Joo
Department of Physics, Korea University
Seoul 136-713 (South Korea)
Fax: (+82) 2-927-3292
E-mail: jjoo@korea.ac.kr
Homepage: http://hynsr.korea.ac.kr
D.-C. Kim, Prof. J. Kim
Department of Physics, University of Incheon
Incheon 406-772 (South Korea)
J. S. Kim, Dr. S. Y. Jang
Polymer Hybrid Center, Korea Institute of Science and Technology
Seoul 136-791 (South Korea)

[**] This work was supported in part by a National Research Foundation of Korea (NRF) grant funded by the Korea government (MEST) (20090071842 and R0A-2007-000-20053-0).

Supporting information for this article is available on the WWW under http://dx.doi.org/10.1002/anie.201007358.

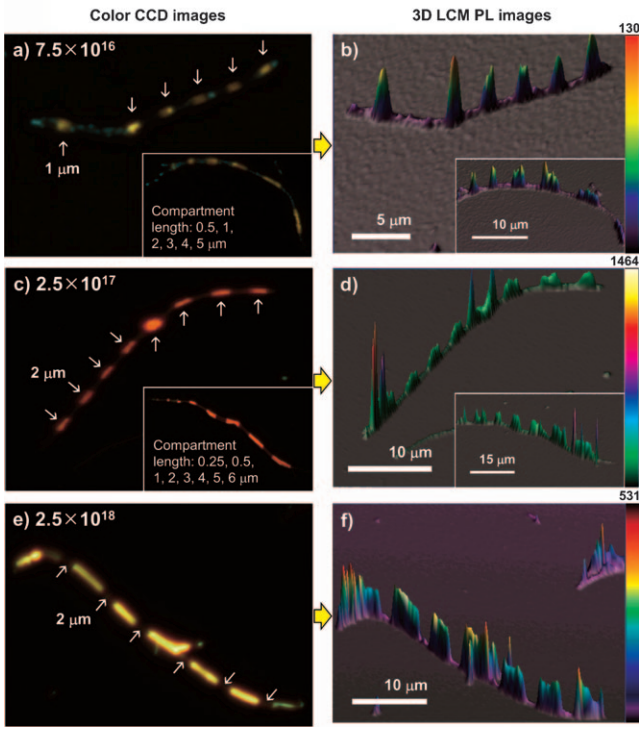

Figure 1. a,b) Color CCD and 3D LCM PL images of a single P3MT NW treated with a focused E-beam (dose = 7.5×10^{16} electrons cm^{-2}). Insets: Corresponding images of a treated P3MT NW with different compartment lengths. c,d) Color CCD and 3D LCM PL images of a single P3MT NW treated with a focused E-beam (dose = 2.5×10^{17} electrons cm^{-2}). Insets: Corresponding images of a treated P3MT NW with different compartment lengths. e,f) Color CCD and 3D LCM PL images of a single P3MT NW treated with a focused E-beam (dose = 2.5×10^{18} electrons cm^{-2}). The arrows in the color CCD images indicate the treated compartments. The color scale bar on the right-hand side represents the photon counts.

compartments changed to bright red (Figure 1c), and a significant increase (ca. 31 times) in the light-emission intensity was confirmed from the LCM PL images (Figure 1d). When the focused E-beam dose was increased to 2.5×10^{18} electrons cm^{-2}, the PL intensity of the treated compartments in the NW decreased, and bright yellow-green emission was observed from the pristine compartments of the same NW (Figure 1e,f). The results indicate the existence of a critical E-beam dose (ED_C) for modification of the optical properties in the P3MT NWs and for E-beam energy transfer along the NWs. Above the ED_C, the focused E-beam energy might be actively transferred toward pristine compartments to change observable optical properties.

The size of the compartments on the P3MT NW treated with the focused E-beam was controlled through the designed patterns (including size and position). In Figure 1a,c, the length of the treated compartments on the NW was 1 and 2 μm, respectively. The length of the treated compartments was also controlled to 0.25, 0.5, 1, 2, 3, 4, 5, and 6 μm in the same NW (inset of Figure 1c). Similar enhancement and color variation of light emission was observed for the treated NW with different compartment lengths (inset Figure 1a,c).

The averaged LCM PL intensities of the NW compartments, obtained from the line profile of three-dimensional (3D) LCM PL images, were changed considerably by the E-beam dose (Figure 2a). The LCM PL intensity of the pristine P3MT NW was six photon counts, and that of the pristine compartments in the treated P3MT NW were 7, (34 ± 1), (265 ± 5), and (326 ± 14) photon counts for doses of 7.5×10^{16}, 2.5×10^{17}, 2.5×10^{18}, and 1.0×10^{19} electrons cm^{-2}, respectively. The LCM PL intensities of the treated NW compartments were (70 ± 3), (185 ± 6), (24 ± 1), and (3 ± 1), respectively, for the doses listed above. The ratios of the LCM PL intensities of the treated to the pristine compartments in the same NW were 10.0 and 5.44 with doses of 7.5×10^{16} and 2.5×10^{17} electrons cm^{-2}, respectively. At high doses of 2.5×10^{18} and 1.0×10^{19} electrons cm^{-2}, the PL intensity ratios of the pristine to the treated compartments were 11.0 and 108.7, thus suggesting the existence of a ED_C and E-beam energy transfer from the treated to pristine compartments. These results are in agreement with the color CCD and 3D LCM PL images shown in Figure 1.

The maximum intensity of the LCM PL spectrum of the pristine P3MT single NW, excluding sharp Raman peaks at 525 and 569 nm,[9] was chosen as a reference (inset of Figure 2b). The LCM PL peak was gradually red-shifted from 520–530 nm for the pristine NW to approximately 560 and 590–600 nm for the NW compartments treated with doses of 7.5×10^{16} and 2.5×10^{17} electrons cm^{-2}, respectively (Figure 2b). The intensities of the LCM PL peaks of the treated compartments with these doses were enhanced up to 25 and 50 times, respectively, with respect to that of the pristine NW. Below the ED_C, the positions and intensities of LCM PL peaks were red-shifted and increased with increasing E-beam dose. However, the emission intensity of the compartments treated with a dose higher than the ED_C (2.5×10^{18} electrons cm^{-2}) was decreased considerably (inset Figure 2b). This finding confirmed the results of the color CCD and LCM PL images. Therefore, the PL color and intensity of the P3MT single NW can be tailored precisely on the nanoscale as a function of the focused E-beam dose.

Figure 2c shows the micro-Raman spectra of the pristine and treated P3MT NW compartments and reveals structural and doping characteristics. Significant differences in micro-Raman spectra associated with the focused E-beam treatment were observed in the range of 1050–1650 cm^{-1}. The intensities of the Raman peaks at 1192, 1223, and 1361 cm^{-1}, corresponding to C_β–H bending, antisymmetric C_α–$C_{\alpha'}$ ring stretching, and C_β–$C_{\beta'}$ ring stretching deformation modes, respectively,[9,10] decreased with increasing E-beam dose. The intensity of the doping-induced Q mode at 1404 cm^{-1} decreased gradually with increasing E-beam dose (see the Supporting Information).[9a] The intensities, positions, and line widths of the Raman peaks at 1457 and 1510 cm^{-1}, corresponding to the disorder mode (D) and the antisymmetric C_α=C_β ring stretching mode (ν_1), respectively,[9a,10,11] were increased, up-shifted, and broadened with increasing E-beam dose. The changes in the D and ν_1 vibration peaks indicate structural modifications of the main polymeric chains in the NW. The spectra reveal that the focused E-beam irradiation induces conformational modification of polymer

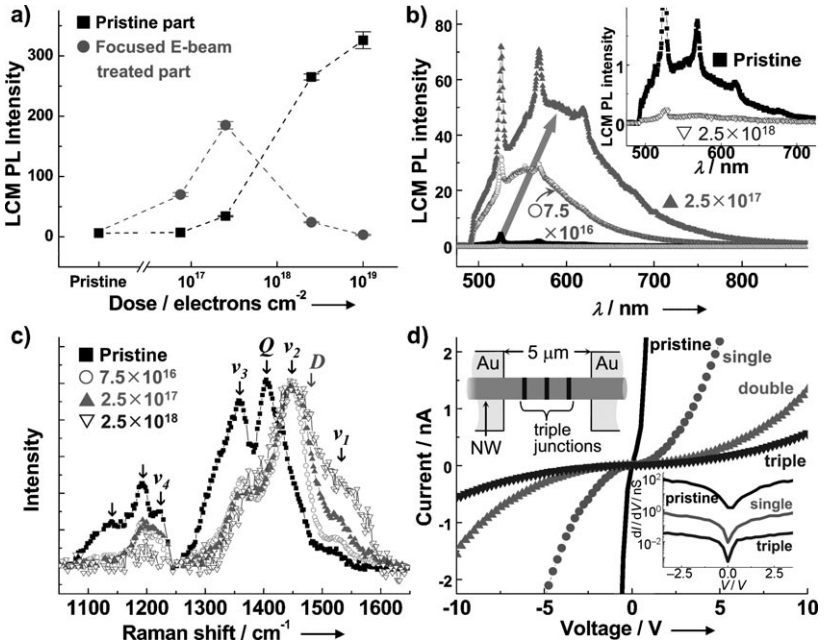

Figure 2. a) Averaged LCM PL intensity of P3MT NW compartments treated with a focused E-beam as a function of dose. b) LCM PL spectra of the pristine P3MT NW compartments and of compartments treated with a focused E-beam at various doses (electrons cm^{-2}). Inset: Magnified LCM PL spectra of the pristine compartments and of the compartments treated with a high dose. c) Normalized micro-Raman spectra for the pristine and treated P3MT NW compartments at various doses. See text for details. d) Comparison of *I–V* characteristic curves of the pristine and treated P3MT single NW with various multiple serial junctions. Top inset: Schematic diagram of the NW with triple junctions on Au electrodes. Bottom inset: Voltage dependence of the differential conductance of the pristine and treated single P3MT NW with various junctions.

chains on the nanoscale and causes a decrease in the doping level of the polymer (see the Supporting Information).[9a]

To examine the effect of the focused E-beam treatment on electrical properties, current–voltage (*I–V*) characteristics were measured for multiple 1D serial junctions of the P3MT single NW, in which single, double, and triple junctions were made in the same NW depending on the number of treatments (top inset of Figure 2d). The dose of the focused E-beam was 1.0×10^{17} electrons cm^{-2}, which was below the ED_C to minimize the E-beam energy transfer effect. As the number of the treated compartments (i.e., junctions) increased, the current levels of the P3MT single NW decreased dramatically, and the nonlinearity of the *I–V* curves became severe (Figure 2d). The results were similar to those reported for heterojunction nanomaterials with multiple 1D serial compartments and superlattice structures.[4a,12] The voltage dependence of differential conductance in the low bias region was reduced and sharpened when the number of junctions was increased (bottom inset of Figure 2d). The results suggest that the treated compartment acts as a tunneling barrier for charge transport.[12a,13]

The focused E-beam irradiation on the TiO_2 single NW was performed using the same methods in the case of the P3MT NW. The same TiO_2 single NW was irradiated with a focused E-beam at three different doses. The PL intensity of the pristine and treated compartments of the NW was clearly distinguishable in the color CCD and 3D LCM PL images (Figure 3a,b). The LCM PL intensities of the treated TiO_2 NW compartments in the single NW increased when the dose was increased from 1.0×10^{17} to 5.0×10^{17} and then to 1.0×10^{18} electrons cm^{-2} (Figure 3b). For a dose of 5.0×10^{18} electrons cm^{-2}, which was higher than ED_C, the PL intensity at both edges of the treated compartments decreased to that of the pristine compartments, thus indicating the E-beam energy transfer effect (insets of Figure 3a,b). The TiO_2 NW was also tailored precisely with 23 periodic serial compartments using a focused E-beam with a dose of 1.0×10^{18} electrons cm^{-2} (Figure 3c,d). The treated NW compartments had an equal length of 2.0 μm and were separated by pristine compartments with a length of 1.5 μm. The LCM PL efficiency of the treated TiO_2 NW compartments was up to 19 times higher than that of the pristine NW (Figure 3d), and periodic luminescence alternation similar to that of a light-emitting barcode NW was detected.[14]

The peak LCM PL spectra of the pristine TiO_2 single NW compartments was detected at approximately 480 nm,[15] which red-shifted gradually from about 500 to about 680 nm when the E-beam dose was increased from 1.0×10^{17} to 5.0×10^{18} electrons cm^{-2} (Figure 3e). The line width of the LCM PL spectrum of the treated NW compartments increased with increasing dose. The average LCM PL intensities of the NW compartments treated with doses of 1.0×10^{17}, 5.0×10^{17}, 1.0×10^{18}, 5.0×10^{18}, and 1.0×10^{19} electrons cm^{-2} were (23 ± 1), (106 ± 2), (148 ± 3), (51 ± 1), and (27 ± 4) photon counts, respectively (Figure 3f). The LCM PL intensities of the treated TiO_2 NW compartments increased rapidly between 1.0×10^{17} and 5.0×10^{17} electrons cm^{-2} (Figure 3f). Similar to the single P3MT NW treated with the E-beam, an ED_C for E-beam energy transfer in the TiO_2 NW might exist between 1.0×10^{18} and 5.0×10^{18} electrons cm^{-2}. The results suggest that the focused E-beam treatment of the TiO_2 NW induced defects, such as vacancies or interstitials, which contributed to the change in optical properties of TiO_2 NW.[5,15,16]

Focused E-beam irradiation of designated positions of the P3MT and TiO_2 NWs at various doses resulted in the nanoscale tailoring of the intrinsic characteristics. We observed that below the ED_C, the PL efficiency of the organic P3MT and inorganic TiO_2 NW compartments treated with the focused E-beam increased with increasing dose. Above the ED_C, the focused E-beam energy was transferred actively to the pristine compartments. The treated compartments in the single P3MT NW acted as a tunneling barrier for charge transport. The results in this study suggest applications to light-emitting nanoscale barcodes, nanoscale optoelectronic devices, and 1D superlattices. Focused E-beam irradiation as

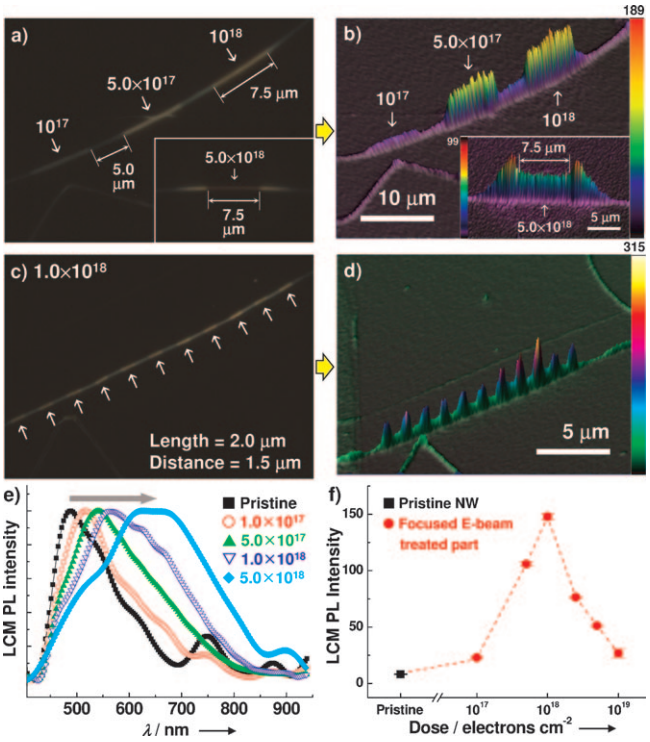

Figure 3. a) Color CCD image of a single TiO_2 NW treated with a focused E-beam at three different doses (given in electrons cm^{-2}). Inset: Color CCD image of the single TiO_2 NW treated with a high dose. b) Corresponding LCM PL images of the same samples. c, d) Color CCD (c) and 3D LCM PL (d) images of the treated TiO_2 NW with 23 compartments. The arrows indicate the compartments treated with the focused E-beam. The color scale bar on the right-hand side represents photon counts. e) Normalized LCM PL spectra of the pristine and treated TiO_2 NW compartments with various doses. f) Averaged LCM PL intensity of the TiO_2 NWs as a function of the dose.

a postsynthesis manipulation procedure is a promising technique for fine tailoring of the intrinsic properties of nanosystems.

Experimental Section

P3MT NWs of approximately 240 nm diameter were fabricated using an electrochemical polymerization method based on an anodic alumina oxide (Al_2O_3) nanoporous template (see the Supporting Information).[9a,17] The anatase TiO_2 NWs of approximately 290 nm diameter were fabricated by electrospinning (see the Supporting Information).[18]

The p-type doped Si or Si/SiO_2 wafers were patterned by photolithography including gold deposition and a lift-off process. The gold layer with the wafers was used as a conducting substrate for the focused E-beam treatment. The shape of the pattern was designed to determine the exact position of the target single NW. After loading the target single NW onto the substrate, the position of the target NW with reference to the Au pattern was examined by optical microscopy. The focused E-beam, generated from a conventional E-beam lithography instrument (Tescan VEGA TS 5130 MM with ELPHY Quantum Pattern Generator), was used to irradiate the intended positions in a single strand of P3MT or TiO_2 NW normal to their length under high-vacuum conditions ($\leq 7.8\times10^{-5}$ torr) at room temperature.

The nanoscale and solid-state PL images and spectra of the single P3MT and TiO_2 NWs were measured using a LCM with 2D (x–y) Piezo-Scanner (E-501 Modular Piezo Controller, Physik Instrument). The PL color CCD images of the single NWs were measured using a cooled CCD color camera (INFINITY3–1C, Lumenera) and mercury arc lamp (see the Supporting Information).[9a,17b] The I–V characteristics for the pristine and treated P3MT NWs were measured using a Keithley 237 SMU at room temperature under moderate vacuum ($\leq 1.0\times10^{-2}$ torr; see the Supporting Information for details).

Received: November 23, 2010
Published online: March 14, 2011

Keywords: electron beams · luminescence · nanostructures · nanotechnology · superlattices

[1] L. Esaki, R. Tsu, *IBM J. Res. Dev.* **1970**, *14*, 61–65.
[2] a) M. S. Gudiksen, L. J. Lauhon, J. Wang, D. C. Smith, C. M. Lieber, *Nature* **2002**, *415*, 617–620; b) R. Yan, D. Gargas, P. Yang, *Nat. Photonics* **2009**, *3*, 569–576; c) R. Tsu, *Superlattice to nanoelectronics*, Elsevier, Amsterdam, **2005**.
[3] a) S. R. Nicewarner-Peña, R. G. Freeman, B. D. Reiss, L. He, D. J. Peña, I. D. Walton, R. Cromer, C. D. Keating, M. J. Natan, *Science* **2001**, *294*, 137–141; b) L. Qin, M. J. Banholzer, J. E. Millstone, C. A. Mirkin, *Nano Lett.* **2007**, *7*, 3849–3853; c) B. S. Williams, *Nat. Photonics* **2007**, *1*, 517–525; d) A. Wade, G. Fedorov, D. Smirnov, S. Kumar, B. S. Williams, Q. Hu, J. L. Reno, *Nat. Photonics* **2009**, *3*, 41–45.
[4] a) M. T. Björk, B. J. Ohlsson, T. Sass, A. I. Persson, C. Thelander, M. H. Magnusson, K. Deppert, L. R. Wallenberg, L. Samuelson, *Nano Lett.* **2002**, *2*, 87–89; b) J. R. Choi, S. J. Oh, H. Ju, J. Cheon, *Nano Lett.* **2005**, *5*, 2179–2183; c) J. H. Lee, J. H. Wu, H. L. Liu, J. U. Cho, M. K. Cho, B. H. An, J. H. Min, S. J. Noh, Y. K. Kim, *Angew. Chem.* **2007**, *119*, 3737–3741; *Angew. Chem. Int. Ed.* **2007**, *46*, 3663–3667; d) R. E. Algra, M. A. Verheijen, M. T. Borgström, L. F. Feiner, G. Immink, W. J. P. Van Enckevort, E. Vlieg, E. P. A. M. Bakkers, *Nature* **2008**, *456*, 369–372; e) A. Bulbarello, S. Sattayasamitsathit, A. G. Crevillen, J. Burdick, S. Mannino, P. Kanatharana, P. Thavarungkul, A. Escarpa, J. Wang, *Small* **2008**, *4*, 597–600; f) P. Caroff, K. A. Dick, J. Johansson, M. E. Messing, K. Deppert, L. Samuelson, *Nat. Nanotechnol.* **2009**, *4*, 50–55.
[5] a) A. V. Krasheninnikov, F. Banhart, *Nat. Mater.* **2007**, *6*, 723–733; b) A. V. Krasheninnikov, K. Nordlund, *J. Appl. Phys.* **2010**, *107*, 071301.
[6] M. D. Fischbein, M. Drndić, *Appl. Phys. Lett.* **2008**, *93*, 113107.
[7] H. M. Lee, Y. N. Kim, B. H. Kim, S. O. Kim, S. O. Cho, *Adv. Mater.* **2008**, *20*, 2094–2098.
[8] E. J. Lee, J. J. Kim, S. O. Cho, *Langmuir* **2010**, *26*, 3024–3030.
[9] a) Y. K. Hong, D. H. Park, S. K. Park, H. Song, D. C. Kim, J. Kim, Y. H. Han, O. K. Park, B. C. Lee, J. Joo, *Adv. Funct. Mater.* **2009**, *19*, 567–572; b) G. Louarn, M. Trznadel, J. P. Buisson, J. Laska, A. Pron, M. Lapkowski, S. Lefrant, *J. Phys. Chem.* **1996**, *100*, 12532–12539.
[10] G. Shi, J. Xu, M. Fu, *J. Phys. Chem. B* **2002**, *106*, 288–292.
[11] F. Chen, G. Shi, J. Zhang, M. Fu, *Thin Solid Films* **2003**, *424*, 283–290.
[12] a) M. H. Devoret, H. Grabert, *Single Charge Tunneling: Coulomb Blockade Phenomena in Nanostructures*, Plenum, **1992**; b) P. Delsing, T. Claeson, K. K. Likharev, L. S. Kuzmin, *Phys. Rev. B* **1990**, *42*, 7439–7449.
[13] A. N. Aleshin, H. J. Lee, S. H. Jhang, H. S. Kim, K. Akagi, Y. W. Park, *Phys. Rev. B* **2005**, *72*, 1532021.

[14] D. H. Park, Y. K. Hong, E. H. Cho, M. S. Kim, D. C. Kim, J. Bang, J. Kim, J. Joo, *ACS Nano* **2010**, *4*, 5155 – 5162.
[15] a) Y. X. Zhang, G. H. Li, Y. X. Jin, Y. Zhang, J. Zhang, L. D. Zhang, *Chem. Phys. Lett.* **2002**, *365*, 300 – 304; b) X. Chen, S. S. Mao, *Chem. Rev.* **2007**, *107*, 2891 – 2959.
[16] Y. Lei, L. D. Zhang, *J. Mater. Res.* **2011**, *16*, 1138 – 1144.
[17] a) D. H. Park, B. H. Kim, M. G. Jang, K. Y. Bae, J. Joo, *Appl. Phys. Lett.* **2005**, *86*, 113116-1–3; b) D. H. Park, M. S. Kim, J. Joo, *Chem. Soc. Rev.* **2010**, *39*, 2439 – 2452.
[18] a) D. Li, Y. Xia, *Adv. Mater.* **2004**, *16*, 1151 – 1170; b) B. H. Lee, M. Y. Song, S. Y. Jang, S. M. Jo, S. Y. Kwak, D. Y. Kim, *J. Phys. Chem. C* **2009**, *113*, 21453 – 21457; c) B. B. Lakshmi, P. K. Dorhout, C. R. Martin, *Chem. Mater.* **1997**, *9*, 857 – 862.

